Chemical Pathway and Kinetics of Phenol Oxidation by Fenton's Reagent

J. A. ZAZO, J. A. CASAS,
A. F. MOHEDANO,
M. A. GILARRANZ, AND
J. J. RODRÍGUEZ*

*Ingeniería Química, Universidad Autónoma de Madrid,
Crta. de Colmenar km 15, 28049 Madrid, Spain*

Phenol oxidation by Fenton's reagent (H_2O_2 + Fe^{2+}) in aqueous solution has been studied in depth for the purpose of learning more about the reactions involved and the extent of the oxidation process, under various operating conditions. An initial phenol concentration of 100 mg/L was used as representative of a phenolic industrial wastewater. Working temperatures of 25 and 50 °C were tested, and the initial pH was set at 3. The H_2O_2 and the Fe^{2+} doses were varied in the range of 500−5000 and 1−100 mg/L, respectively, corresponding to 1−10 times the stoichiometric ratio. A series of intermediates were identified, corresponding mainly to ring compounds and short-chain organic acids. Most significant among the former were catechol, hydroquinone, and *p*-benzoquinone; the main organic acids were maleic, acetic, oxalic, and formic, with substantially lower amounts of muconic, fumaric, and malonic acids. Under milder operating conditions (H_2O_2 and Fe^{2+} at lower concentrations), a great difference was found between the measured total organic carbon (TOC) and the amount of carbon in all analyzed species in the reaction medium. This difference decreased as the doses of H_2O_2 and Fe^{2+} increased, indicating that the unidentified compounds must correspond to oxidation intermediates between phenol and the organic acids. To establish a complete oxidation pathway, experiments were carried out using each of the identified intermediates as starting compounds. Dihydroxybenzenes were identified in the earlier oxidation stages. Muconic acid was detected in catechol but not in the hydroquinone and *p*-benzoquinone oxidation runs; the last two compounds were oxidized to maleic acid. Oxalic and acetic acid appeared to be fairly refractory to this oxidation treatment. A detailed knowledge of the time evolution of the oxidation intermediates is of environmental interest particularly in the case of hydroquinone and *p*-benzoquinone because their toxicities are several orders of magnitudes higher than that of phenol itself. The time evolution of the intermediates and TOC was fitted to a simple second-order kinetic equation, and the values of the kinetic constants were determined. This provides a simplified approach useful for design purposes.

* Corresponding author phone: +34 91 497 4048; fax: +34 91 497 3516; e-mail: juanjo.rodriguez@uam.es.

1. Introduction

Increasing concern about environmental and health risks demands a more rigorous control of industrial wastewaters, promoting the development and implementation of new treatment technologies capable to deal with toxic pollutants resistant to the widely established conventional methods. Among this type of pollutants, phenol and phenolic compounds have attracted much attention in the last two decades. This interest arises from their relative frequency in the aqueous effluents of the chemical industry. Moreover, phenol is considered to be an intermediate in the oxidation pathway of high molecular weight aromatic hydrocarbons, and thus it is frequently used as a model compound for advanced wastewater studies (*1*).

Advanced oxidation processes (AOPs) are an interesting treatment option for this type of wastewaters, because of their great potential to oxidize, partially or totally, numerous organic compounds (*2−4*). These processes are based on the generation of hydroxyl radicals (OH•). This species is a more powerful oxidant (*E*° 2.8 V) than the chemical reagents commonly used for this purpose, such as ozone (*E*° 2.0 V) or H_2O_2 (*E*° 1.8 V). Rate constants in AOPs for organic compounds are several orders of magnitude higher than those reported for others processes such as ozonation (*5, 6*). Due to its high reactivity, the hydroxyl radical is very unstable and must be continuously produced in situ by means of chemical or photochemical reactions (*3*). The main methods to generate this radical consist of the use of O_3 at elevated pH (>8.5), O_3/H_2O_2, O_3/catalyst, Fenton's Reagent (Fe^{2+}/H_2O_2), O_3/UV, H_2O_2/UV, O_3/H_2O_2/UV, photo-Fenton/Fenton-like systems, and photocatalytic oxidation (UV/TiO_2) (*7*).

One of the most effective AOPs consists of the use of Fenton's reagent, a combination of H_2O_2 and Fe^{2+}. In this process, H_2O_2 decomposes catalytically by means of Fe^{2+} at acid pH, giving rise to hydroxyl radicals

$$Fe^{2+} + H_2O_2 \xrightarrow{H^+} Fe^{3+} + OH^\bullet + OH^- \qquad (1)$$
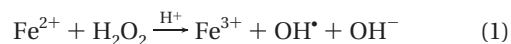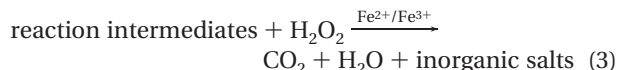
The optimal pH range falls between 3 and 3.5 (*8−10*), although different values have been also reported. Kwon et al. (*11*) obtained similar results at pH values in the range of 2−4. Basu and Wei (*12*) reduced the optimal interval to 2.5−3, whereas Kavitha and Palanivelu (*13*) obtained the highest conversions of chlorophenols at pH values in the range of 2.5−4.

The application of Fenton's reagent as an oxidant for wastewater treatment is attractive, in principle, due to the fact that Fe is a widely available and nontoxic element, and hydrogen peroxide is easy to handle and the excess decomposes to environmentally safe products (*9*). Among the advantages of Fenton's process relative to other oxidation techniques are the simplicity of equipment and the mild operation conditions (atmospheric pressure and room temperature); mainly for these reasons Fenton's process has been regarded as the most economical alternative (*14, 15*).

Numerous authors (*8, 12, 16−19*) have studied the mechanism of oxidation of phenolic compounds by Fenton's reagent. The number of reactions is high, and the schemes of reaction are generally complex. In an overall view, the process can be represented by the following reactions (*20*)

$$COD + H_2O_2 \xrightarrow{Fe^{2+}/Fe^{3+}} \text{reaction intermediates} \qquad (2)$$

reaction intermediates $+ H_2O_2 \xrightarrow{Fe^{2+}/Fe^{3+}}$
$$CO_2 + H_2O + \text{inorganic salts} \quad (3)$$

The oxidation of the substrate completely to CO_2 becomes, in general, uneconomical due to high H_2O_2 consumption. Thus, this process has been mostly proposed as a pretreatment to reduce the effluent toxicity to safe levels for further biological treatment [21]. For this reason, it is necessary to study the reaction pathway in depth, as the toxicity of some intermediates can be higher than that of the initial compound. This is the case in the oxidation of phenol, where hydroquinone and *p*-benzoquinone are formed, the toxicities of which are several orders of magnitude higher than that of phenol itself [22].

Due to the complexity of the whole process, the various reaction schemes found in the literature refer to partial studies, with specific objectives. For some of them, the aim was to detect the reaction intermediates [8, 12], whereas others studied the influence of these products in the evolution of the process. Chen and Pignatello [16] analyzed the role of quinones in the Fe^{3+}/Fe^{2+} redox cycle in phenol oxidation. Kang et al. [18] paid particular attention to the interaction of the organic intermediates with the Fe species, studying their role in the regeneration and in the scavenging of the catalyst. The experimental conditions used in those studies are fairly different. The H_2O_2 to substrate ratio varied between 2 and 6, which is lower than the stoichiometric amount required to complete the oxidation to CO_2. Moreover, the aforementioned studies focus on the early stages of the process.

The aim of the present work is to elucidate a complete route of oxidation of phenol with Fenton's reagent. First, the intermediates from phenol oxidation were identified, using different concentrations of catalyst (Fe^{2+}) and oxidant (H_2O_2). Oxidation runs have been carried out, employing the previously identified intermediates as starting compounds, under similar operating conditions, to follow the complete phenol oxidation pathway. Finally, a kinetic study was carried out, to obtain the kinetic rate constants for the oxidation of each individual intermediate as well as for the overall total organic carbon (TOC).

2. Experimental Section

Experiments were carried out in 100 mL glass batch reactors shaken in a constant-temperature bath at an equivalent stirring velocity around 200 rpm for 4 h. The reaction volume was 50 mL, and the reactants were added simultaneously at the beginning of each run. Temperature was set at 25 and 50 °C. The starting concentrations were 100 mg/L for target compounds and 500 mg/L for H_2O_2, which corresponds to the stoichiometric amount of H_2O_2 necessary to oxidize phenol to CO_2 and H_2O. In phenol oxidation runs, 2500 and 5000 mg/L of H_2O_2 (5 and 10 times the stoichiometric amount) were also tested. The Fe^{2+} dose was varied between 1 and 100 mg/L for the 25 °C runs and between 1 and 10 mg/L for those performed at 50 °C. The initial pH value was 3.0. Under these conditions, when H_2O_2 was used as an oxidant in the absence of Fe^{2+}, oxidation of the starting compound was always negligible.

The samples were analyzed immediately after the reaction. Phenol and aromatic intermediates were identified and quantified by means of high-performance liquid chromatography (HPLC; Varian Pro-Start 240) using a diode array detector (330 PDA). A Microsorb C18 5 μm column (MV 100, 15 cm in length, 4.6 mm in diameter) was used as the stationary phase and 1 mL/min of 4 mM aqueous sulfuric solution as the mobile phase. A UV detector was used at a wavelength of 210 nm for phenol, catechol, and hydroquinone
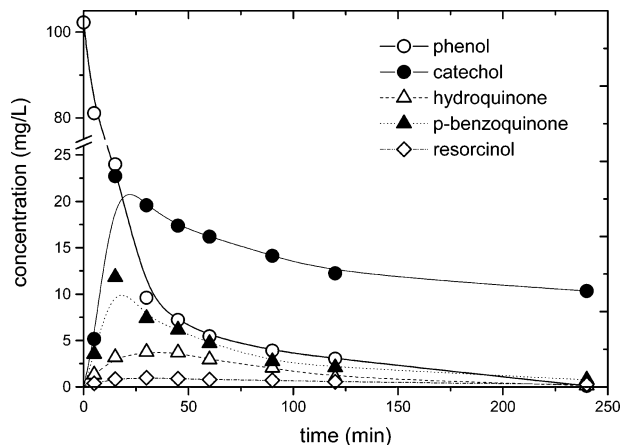

FIGURE 1. Evolution of aromatic compounds identified in phenol oxidation with Fenton's reagent (100 mg/L phenol, 500 mg/L H_2O_2, 1 mg/L Fe^{2+}, 25 °C, pH_0 3).
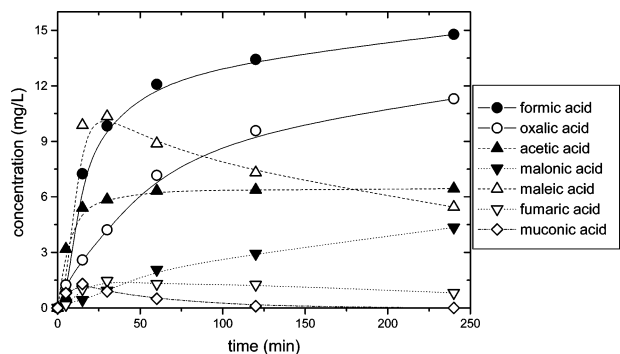

FIGURE 2. Evolution of organic acids identified in phenol oxidation with Fenton's reagent (100 mg/L phenol, 500 mg/L H_2O_2, 1 mg/L Fe^{2+}, 25 °C, pH_0 3).

and at 254 nm for *p*-benzoquinone. Short-chain organic acids were analyzed by means of an ion chromatograph with chemical suppression (Metrohm 790 IC) using a conductivity detector. A Metrosep A supp 5-250 column (25 cm in length, 4 mm in diameter) was used as the stationary phase and 0.7 mL/min of an aqueous solution of 3.2 mM Na_2CO_3 and 1 mM $NaHCO_3$ as the mobile phase. TOC was measured with an OI TOC analyzer (model 1010). Previously, the samples were acidified with phosphoric acid (1 M) to remove carbon from carbonates and bicarbonates. The amount of CO_2 obtained was measured with an infrared detector. The residual H_2O_2 concentration was determined by colorimetric titration using the titanium sulfate method [23].

3. Results and Discussion

3.1. Oxidation Products. Figures 1 and 2 summarize the evolution of the oxidation reaction of phenol with Fenton's reagent. As can be seen, under these experimental conditions close to 90% of phenol is converted in about 30 min, giving rise to dihydroxybenzenes upon hydroxylation of the aromatic ring. Catechol is the main primary oxidation product, indicating that hydroxylation takes place predominantly in the ortho position. The peak concentration of hydroquinone (para-hydroxylation) was about one-tenth that of catechol, whereas resorcinol (meta-hydroxylation) was present only in trace amounts. This situation relative to the distribution of the aromatic oxidation products was similar under all the experimental conditions tested.

Dihydroxybenzenes and benzoquinones are in redox equilibrium in acid media [24], which explains the presence of *p*-benzoquinone. However, it was not possible to dem-
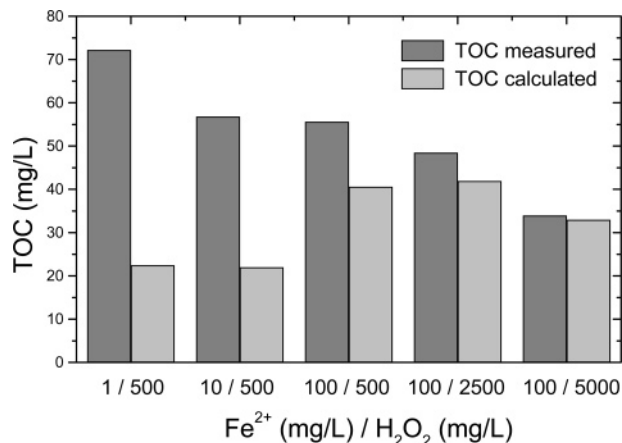
FIGURE 3. Measured and calculated TOC values at different Fe^{2+} and H_2O_2 doses after 4 h of reaction time.

TABLE 1. Elemental Analysis of the Solid Residue Obtained in Phenol Oxidation by Fenton's Reagent

element	C	H	N	S	Fe	O[a]
% weight	46.06	3.04	0.04	3.32	7.96	39.6

[a] By difference.

onstrate the formation of *o*-benzoquinone because this compound is unstable in aqueous solution and there are no commercial standards.

Ring-opening of the aromatic intermediates leads to the formation of organic acids. As a result, a pH decrease takes place, although it remained always within the optimum range, above 2. These compounds are intermediates and/or final oxidation products. Maleic, acetic, and formic acids were the earlier and more abundant products of the acid formation stage. Oxalic acid was appearing at a lower rate, although it reached a high relative concentration as the oxidation reaction proceeded. Maleic and muconic acids show peak concentrations, although the second always remained at a very low concentration. Both are dicarboxylic acids, and the larger ones among the organic acids identified. It can be postulated that these two compounds are the primary products from ring-opening of the aromatic intermediates; they give rise to the short-chain acids in the reaction pathway. Muconic acid was only detected under mild experimental conditions. Malonic and fumaric acids were detected in trace amounts, whereas acetic and oxalic acids were found to be refractory to Fenton's reagent, in agreement with the findings of other authors (*2*, *11*).

However, the high difference found between the measured TOC values and the amount of carbon computed from the identified intermediates and the residual phenol, under the operating conditions of the aforementioned experiment (Figure 3), must be noted. This difference decreased substantially with increasing Fe^{2+} and H_2O_2 doses. At 100 mg/L Fe^{2+} and 5000 mg/L H_2O_2 (10 times the stoichiometric amount) TOC and C from all the identified species were almost balanced. Under these conditions, only oxalic and acetic acid were detected in the reaction medium.

Consistent with these results, unidentified compounds must correspond to oxidation intermediates between phenol and the organic acids. They could be, at least in part, responsible for the dark brown color of the liquid phase during the early stages of the oxidation process, since the color of an aqueous solution prepared with the identified intermediates at the measured concentrations was much lighter. Moreover, once aromatic intermediates were depleted, the liquid became light yellow, probably due to the
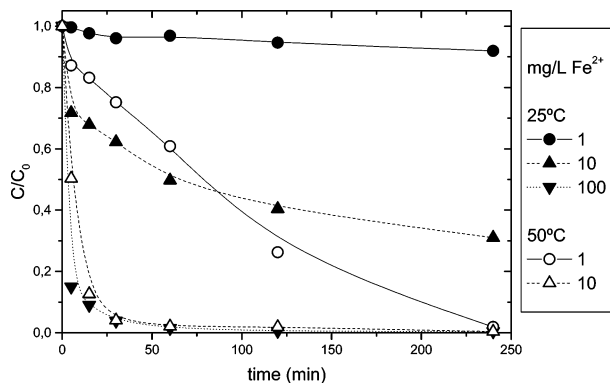

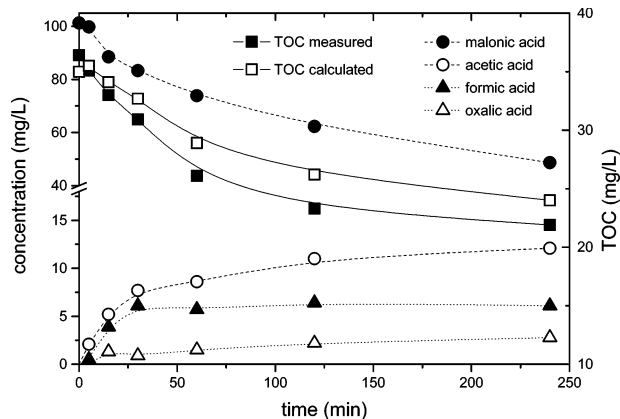FIGURE 4. Experimental results of formic acid oxidation with Fenton's reagent (100 mg/L formic acid, 500 mg/L H_2O_2).

FIGURE 5. Malonic acid oxidation with Fenton's reagent (100 mg/L Fe^{2+}, 500 mg/L H_2O_2, 25 °C).

formation of ferric oxalate. According to Eisenhauer (*25*), the unidentified compounds could be, at least in part, Fe–aromatics complexes. In this group could be also included two-ring compounds (*12*) and, in general, ring condensation products. The presence of a brown solid, after evaporation of the reaction liquid, confirmed this assumption. This solid was insoluble under the experimental conditions (pH 3) but soluble in 1 N aqueous NaOH. Characterization of this solid was performed by elemental analysis and by X-ray fluorescence for Fe. The results are shown in Table 1. The amount of sulfur detected comes from the $FeSO_4$ used as the source of Fe^{2+}. These condensation products were oxidized to oxalic acid at high iron doses and to formic acid when both high iron and H_2O_2 doses were used.

3.2. Route of Phenol Oxidation. To elucidate the oxidation route of phenol by Fenton's reagent, a series of runs were carried out using the identified intermediates as starting compounds (100 mg/L). Previously, the oxidation of these compounds with H_2O_2 in the absence of catalyst (Fe^{2+}) was checked and found negligible.

3.2.1. Evolution of Organic Acids. In the case of formic acid, conversion increased with temperature and Fe^{2+} concentration. As can be seen in Figure 4, it is possible to achieve the complete oxidation of formic acid after 4 h at 50 °C, even at 1 mg/L Fe^{2+}. However, it must be remarked that the initial H_2O_2 concentration was 500 mg/L, which corresponds to 14 times the stoichiometric amount required to oxidize formic acid to CO_2. No intermediates were detected, and the removal of TOC was practically coincident with the amount of carbon corresponding to the converted formic acid, thus confirming that it was oxidized to CO_2.

In the experiments carried out with oxalic acid, no oxidation of this compound was observed at 25 °C, even when using 100 mg/L of Fe^{2+}. These results are in agreement
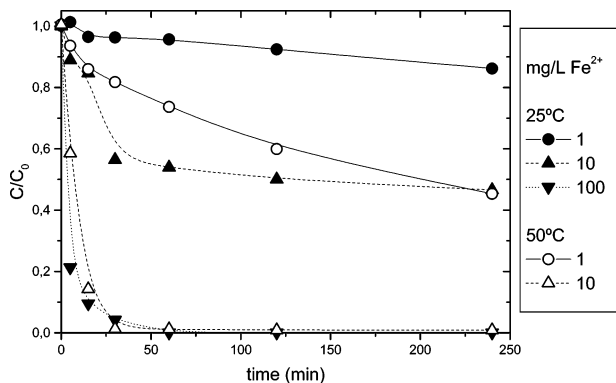
FIGURE 6. Maleic acid oxidation with Fenton's reagent (100 mg/L maleic acid, 500 mg/L H₂O₂).
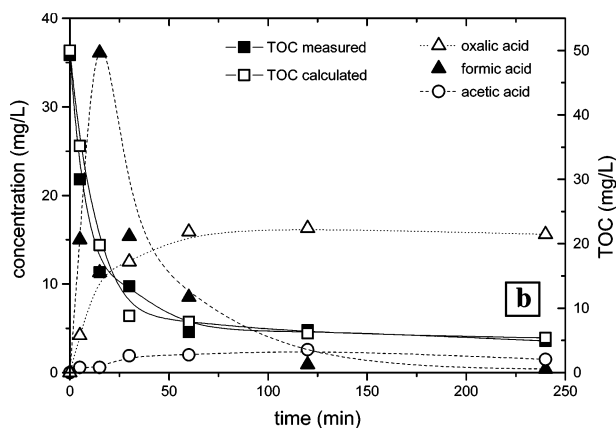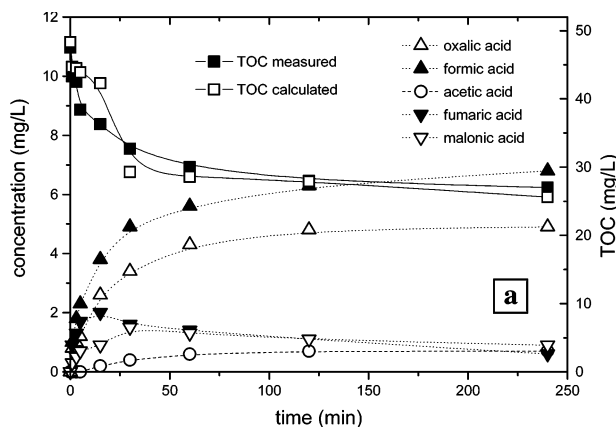

FIGURE 7. Products distribution from maleic acid oxidation with Fenton's reagent at (a) 25 °C and (b) 50 °C; 10 mg/L Fe²⁺, 500 mg/L H₂O₂.

with those obtained in the phenol oxidation runs, in which the oxalic acid concentration remained constant once it reached a maximum value, although the remaining H_2O_2 concentration was always higher than 500 mg/L. However, a conversion of 30% was obtained at 50 °C using 10 mg/L of Fe^{2+}. In any case, intermediates were not found, and C was almost completely balanced. Alegría et al. (26) have proposed a scheme for oxalic acid oxidation with Fenton's reagent that includes the formation of Fe(II) and Fe(III) complexes.

Acetic acid oxidation was negligible (less than 5%), increasing slightly when temperature and catalyst dose were increased. As for the previous compounds, no intermediates were detected, and the amount of carbon in acetic acid was very close to the measured TOC.

Malonic acid appeared in phenol oxidation runs only in trace amounts. Figure 5 shows the results obtained in the
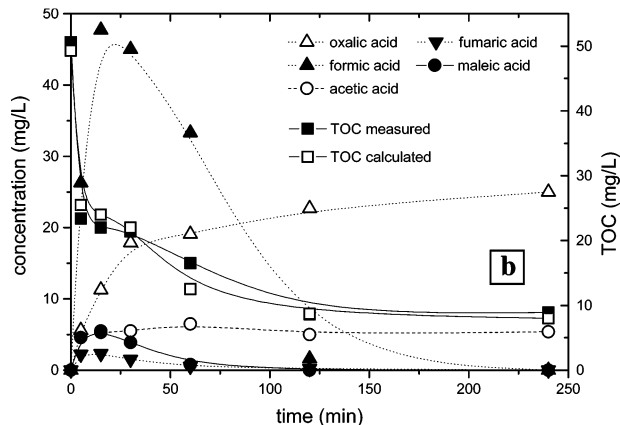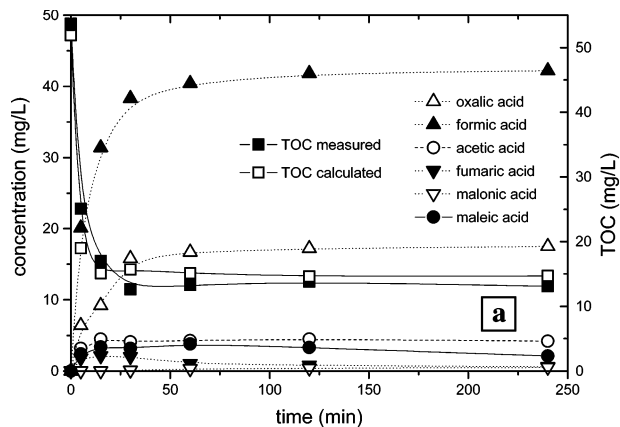
FIGURE 8. Products distribution from muconic acid oxidation with Fenton's reagent at (a) 25 °C and (b) 50 °C; 10 mg/L Fe²⁺, 500 mg/L H₂O₂.

oxidation of this acid with Fenton's reagent. It was mainly oxidized to acetic acid, formic and oxalic acid being also formed. Moreover, the values of TOC and the amount of carbon in the identified intermediates were fairly coincident. Therefore, the reaction scheme proposed for this acid is

$$HOOC-H_2C-COOH \xrightarrow{\quad OH\cdot \quad} H_3C-COOH \quad (4)$$
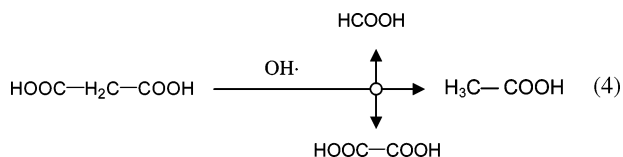
In the case of maleic acid, a complete conversion can be achieved, depending on the operating conditions (Figure 6). At 25 °C, almost 100% of maleic acid is converted after 1 h, using 100 mg/L Fe^{2+}, whereas TOC reduction was 88%. At 50 °C, a practically complete conversion is reached in about 1 h with 10 mg/L of Fe^{2+}, the TOC reduction being close to 90%. With respect to the products distribution (Figures 7a and 7b), formic, oxalic, and acetic acids were detected at both temperatures whereas fumaric acid and traces of malonic acid were also found at 25 °C (Figure 7a). The route for maleic acid oxidation can be postulated as follows
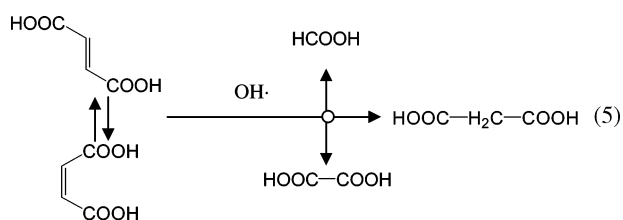
Oxidation to formic acid is the main and the fastest route. At 25 °C, formic acid concentration increased with catalyst concentration but did not reach a maximum value after 4 h of reaction. However, a higher formic acid concentration (37 mg/L) was obtained at 50 °C, which began to decrease as the Fe^{2+} dose increased. Under these conditions, this acid was also completely oxidized to CO_2. Formic acid oxidation began once maleic acid had been depleted, indicating the selectivity of $OH^{\bullet}$ for maleic acid. The production rate of oxalic acid from maleic acid was lower than that for formic acid. Oxalic acid concentration increased with temperature and Fe^{2+} dose. It reached a maximum value of 20 mg/L and then remained constant, in agreement with what was observed in the phenol oxidation experiments. The malonic acid route is the least important. This acid was detected only in the runs performed at 25 °C. However, at 50 °C, acetic acid, but no malonic acid, was detected. Therefore, under these conditions the rate of acetic acid production must be similar to that of malonic acid disappearance. Malonic acid generation from maleic acid was always very low. As can be seen in Figure 7, the amount of carbon from the identified intermediates coincides with the measured TOC, which supports the proposed reaction pathway for maleic acid oxidation.

Among the organic acids, muconic acid showed the highest oxidation rate. It was possible to reach its total depletion in a few minutes even under mild conditions (25 °C and 10 mg/L Fe^{2+}). The oxidation of this compound yielded maleic, fumaric, oxalic, formic, and acetic acids. Malonic acid was only detected in the runs performed at 25 °C (Figure 8).

The first step in muconic acid oxidation consists of $OH^{\bullet}$ attack at the double bonds, yielding maleic acid, which is further oxidized according to the already presented oxidation scheme.

$$
\text{(6)}
$$
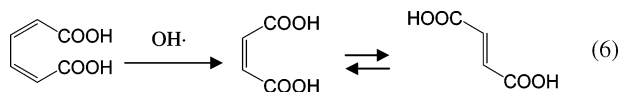
3.2.2. Evolution of Aromatic Intermediates. In the catechol oxidation experiments, aromatic intermediates were not detected. However, in the HPLC chromatograms an unidentified peak appeared next to that of *p*-benzoquinone. Its UV spectrum was similar to that of *p*-benzoquinone but with a maximum at a wavelength of 255 nm. According to Scott (*27*), this compound could be *o*-benzoquinone, although it could not be confirmed because standards are not commercially available.

Figure 9 shows the results from catechol oxidation. The main products were maleic, acetic, oxalic, and formic acids. Muconic, fumaric, and malonic acids were detected only in trace amounts during the first minutes of reaction under very mild experimental conditions (1 mg/L Fe^{2+}, 25 °C). According to Jones (*9*), muconic acid is the primary product from catechol oxidation. Potter and Roth (*8*) proposed a reaction scheme for catechol oxidation with Fenton's reagent that proceeds through the formation of ferric catecholate, which is oxidized to ferric hydroperoxicatecholate and then to *cis,cis*-muconic acid. The remainder of the aforementioned acids result from muconic acid oxidation.

As previously reported for phenol, a great difference between measured and calculated TOC was observed in catechol oxidation (Figure 9a). This fact indicates the presence of unidentified products. Moreover, the color of the liquid phase was also strongly brown during the early reaction stages and became light brown as the aromatics concentration decreased. However, it is important to notice that in the oxidation of organic acids the liquid remained colorless or lightly yellow, most probably due to ferric oxalate. In these last runs, the carbon balance was always closely satisfied.
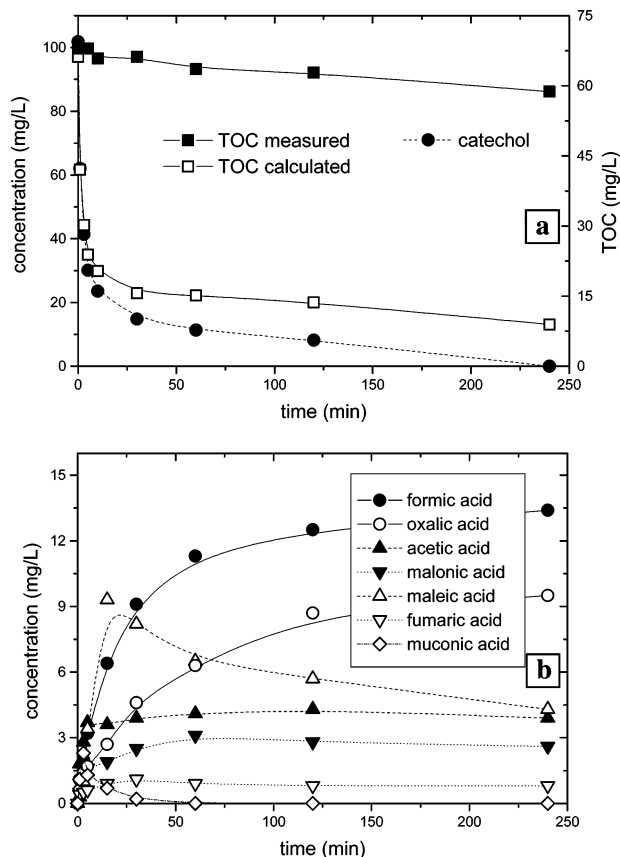

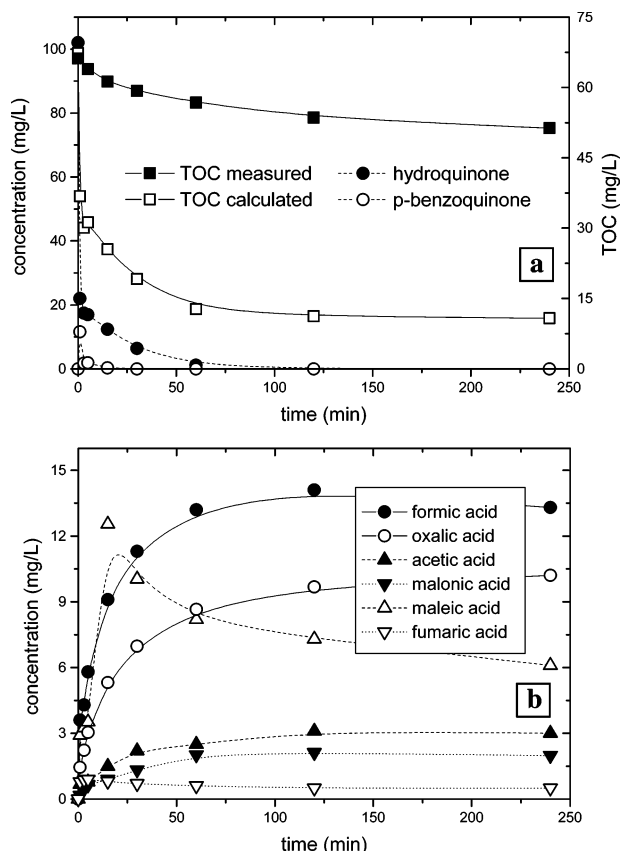**FIGURE 9.** (a) Catechol oxidation and (b) products distribution; 1 mg/L Fe^{2+}, 500 mg/L H_2O_2, 25 °C.

FIGURE 10. (a) Hydroquinone oxidation and (b) products distribution; 1 mg/L Fe^{2+}, 500 mg/L H_2O_2, 25 °C.
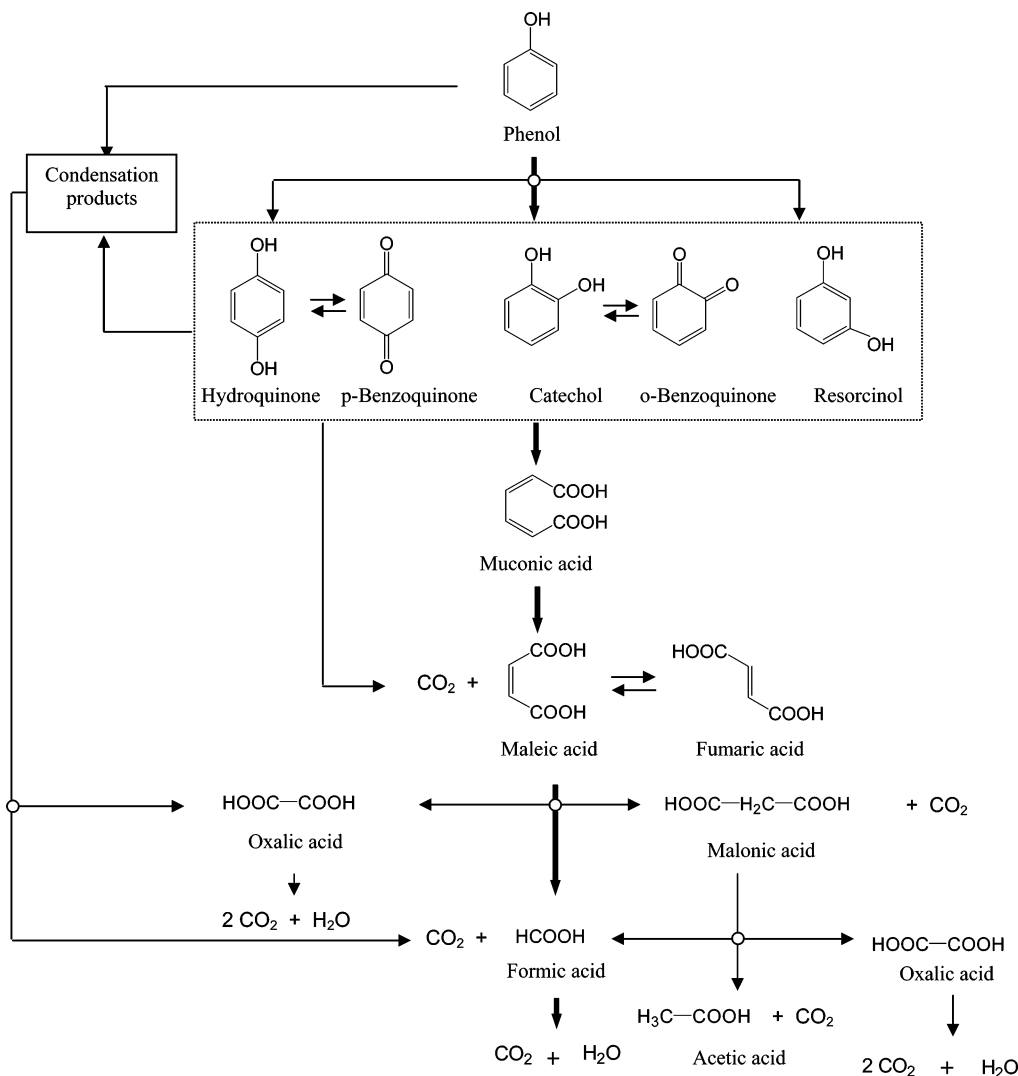
FIGURE 11. Proposed route for phenol oxidation by Fenton's reagent.

Therefore, the unidentified compounds must be condensation or polymerization products from aromatic or quinone compounds and Fe—aromatic complexes, such as ferric catecholate.

The hydroquinone and *p*-benzoquinone oxidation routes were very similar. As already indicated, both compounds are in redox equilibrium. Figure 10 shows the results obtained for hydroquinone. Maleic, oxalic, and formic acids were the main oxidation products identified. Fumaric and acetic acids were found in low concentrations. Malonic acid was detected in the experiments carried out at 25 °C, but not at 50 °C. However, muconic acid was never detected. Thus, maleic acid must be the primary intermediate from ring-opening of hydroquinone and *p*-benzoquinone. Scheck and Frimmel (*28*) came to the same conclusion. They proposed the cleavage of the hydroquinone double bond upon hydroxylation to give maleic and oxalic acids. Again, a great difference between measured and calculated TOC was observed. However, the brown color of the liquid phase was not as dark as that for phenol and catechol oxidation. Probably, the Fe—hydroquinone complex is not formed, and the unidentified compounds are now just condensation or polymerization products from aromatic or quinone compounds.

Figure 11 summarizes the scheme of reaction proposed for phenol oxidation with Fenton's reagent, according to our results.

As can be seen, phenol oxidation by Fenton's reagent proceeds initially through hydroxylation of the aromatic ring to yield dihydroxybenzenes, mainly catechol and hydroquinone, which are in redox equilibrium with benzoquinones. Ring-opening of catechol gives rise to muconic acid, which is further oxidized to maleic and fumaric acids. However, muconic acid is not detected in hydroquinone and *p*-benzoquinone oxidation, where maleic acid is the primary product from ring cleavage. All of the intermediates are finally oxidized to formic acid and oxalic acid, when high Fe^{2+} and H_2O_2 concentrations are used. Under these conditions, formic acid is also oxidized to CO_2 and H_2O, whereas oxalic acid shows quite refractory behavior and remains in solution.

3.3. Kinetics of Phenol and Intermediates Oxidation. The time—concentration curves obtained from the oxidation experiments of phenol and of each individual intermediate were fitted to a potential kinetic equation. In the case of organic acids, the oxidation rate can be described by pseudo-second-order kinetics, provided that the concentration of OH⁻ can be considered constant (eq 7). As these compounds are not able to regenerate the catalyst, it is necessary to use a high Fe^{2+} concentration.

$$-r_A = kC_A{}^2C_{OH\cdot} \cong k'C_A{}^2 \qquad (7)$$

The values obtained for the kinetic constants at 25 °C using 100 mg/L Fe^{2+} and 500 mg/L of H_2O_2 and a 100 mg/L initial concentration of organic acid are summarized in Table 2. In the case of muconic acid, an Fe^{2+} dose of 10 mg/L was used,

TABLE 2. Kinetic Constant Values for Phenol Oxidation Route at 25 °C

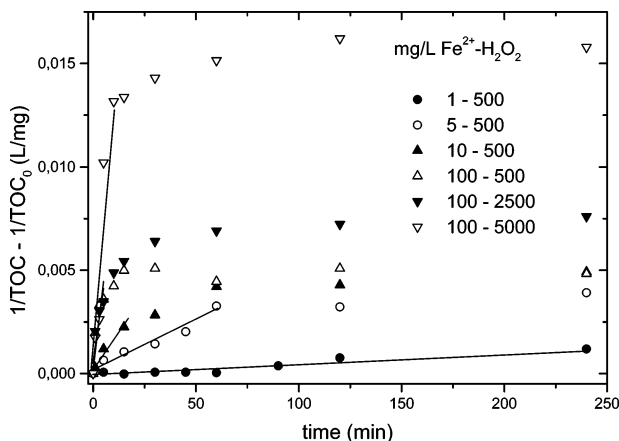| compound	Fe^{2+} (mg/L)	k' (L/(mmol min))	r
formic acid	100	0.479 ± 0.007	0.999
malonic acid		$4.6 \times 10^{-3} \pm 2.5 \times 10^{-3}$	0.992
maleic acid		0.909 ± 0.041	0.996
muconic acid	10	1.16 ± 0.14	0.986
aromatics	1	0.032 ± 0.001	0.993
	5	5.92 ± 0.37	0.994
	10	22.86 ± 2.06	0.991

FIGURE 12. Fitting of TOC evolution to a second-order reaction kinetic model using different Fe^{2+} and H_2O_2 concentrations at 25 °C (TOC_0 76.6 mg/L).

due to its high oxidation rate. The oxidation rate follows the sequence

muconic acid > maleic acid > formic acid > malonic acid

According to these results, the number of double bonds of the organic acid molecule seems to affect the oxidation rate.

The aromatic intermediates showed a higher oxidation rate than the organic acids and also than phenol. These aromatic intermediates can reduce Fe^{3+} to Fe^{2+} (*16*), which enhances significantly the $OH^{\bullet}$ generation, thus increasing the oxidation rate. The kinetic models found in the literature (*16*, *18*, *19*) are fairly complex, including a large number of reactions to describe the interactions among the organic (initial compounds and breakdown intermediates) and inorganic species involved.

However, the evolution of the aromatic species lumped together can be also described by a pseudo-second-order kinetic (eq 7). Due to the ability of these compounds to regenerate the catalyst, the concentration of $OH^{\bullet}$ can be considered constant at different initial Fe concentrations. Table 2 shows the kinetic constant values obtained at 25 °C using 100 mg/L phenol initial concentration and the stoichiometric amount of H_2O_2 at different Fe^{2+} doses. No data were obtained at 100 mg/L Fe^{2+} because, under this condition, aromatics were not detected after 1 min of reaction time.

A similar second-order kinetic equation has been used to fit the time evolution of TOC in phenol oxidation with Fenton's reagent. However it is applicable only up to a certain reaction time (Figure 12). As oxidation proceeds, finally the TOC reaches a plateau value that depends of the operating conditions. As indicated before, the higher the H_2O_2 and the Fe^{2+} amounts, the lower the residual TOC (Figure 3). Under the most severe conditions, only acetic and oxalic acids remain in the reaction medium as oxidation products whereas under milder conditions a variable amount of the remaining

TABLE 3. Kinetic Constant Values Based on TOC at 25 °C

TOC (mg/L)	H_2O_2 (mg/L)	Fe^{2+} (mg/L)	k' (L/(mg min))	r
76.6	500	1	$6.05 \times 10^{-6} \pm 1.0 \times 10^{-6}$	0.968
		5	$4.84 \times 10^{-5} \pm 4.2 \times 10^{-6}$	0.989
		10	$1.45 \times 10^{-4} \pm 2.1 \times 10^{-5}$	0.987
		100	$1.04 \times 10^{-3} \pm 3.4 \times 10^{-4}$	0.963
	2500		$9.37 \times 10^{-4} \pm 3.8 \times 10^{-4}$	0.937
	5000		$1.38 \times 10^{-3} \pm 2.6 \times 10^{-4}$	0.954

TOC corresponds to unidentified species, most probably in a great part ring condensation products, as already discussed. The values obtained for the apparent second-order kinetic constant based on TOC are given in Table 3.

The oxidation rate is related with the initial Fe^{2+} doses, as it can be appreciated from the increase of the kinetic constant value reported in Table 2 for aromatics. Nevertheless, a proportional relationship between the kinetic constant and the initial Fe^{2+} dose does not exist. In the case of TOC (Table 3), it is possible to establish such a relationship.

$$(-r_{TOC}) \cong k(TOC)^2$$
$$k \, (L/(mg\ min)) \cong 1.01 \times 10^{-5} C_{Fe}(mg/L) \quad (8)$$

The final TOC conversion, after 4 h of reaction time, depends on the H_2O_2 concentration as can be seen from Figure 3, but this variable hardly affects to the oxidation rate, as can be appreciated from the kinetic constant values at different initial H_2O_2 concentrations.

Literature Cited

(1) Ding, Z.; Aki, S.; Abraham, M. A. Catalytic supercritical water oxidation: Phenol conversion and product selectivity. *Environ. Sci. Technol.* **1995**, *29* (11), 2748−2753.

(2) Bigda, R. J. Consider Fenton's chemistry for wastewater treatment. *Chem. Eng. Prog.* **1995**, *91* (12), 62−66.

(3) Esplugas, S.; Giménez, J.; Contreras, S.; Pascual, E.; Rodríguez, M. Comparison of different advanced oxidation processes for phenol degradation. *Water Res.* **2002**, *36* (4), 1034−1042.

(4) Neyens, E.; Baeyens, J. A review of classic Fenton's peroxidation as an advanced oxidation technique. *J. Hazard. Mater.* **2003**, *98*, 33−50.

(5) De Laat, J.; Gallard, H.; Ancelin, S.; Legube, B. Comparative study of the oxidation of atrazine and acetone by H_2O_2/UV, Fe(III)/H_2O_2/UV and Fe(II) or Fe(III)/H_2O_2. *Chemosphere* **1999**, *39* (15), 2693−2706.

(6) Benitez, F. J.; Beltran-Heredia, J.; Acero, J. L.; Rubio, F. J. Oxidation of several chlorophenolic derivatives by UV irradiation and hydroxyl radicals. *J. Chem. Technol. Biotechnol.* **2001**, *76* (3), 312−320.

(7) Munter, R. Advanced oxidation processes. Current status and prospects. *Proc. Est. Acad. Sci., Chem.* **2001**, *50* (2), 59−80.

(8) Potter, F. J.; Roth, J. A. Oxidation of chlorinated phenols using Fenton's reagent. *Hazard. Waste Hazard. Mater.* **1993**, *10* (2), 157−170.

(9) Jones, C. W. *Applications of Hydrogen Peroxide and Derivatives*; Royal Society of Chemistry: Cambridge, U. K., 1999.

(10) Goi, A.; Trapido, M. Hydrogen peroxide photolysis, Fenton reagent and photo-Fenton for the degradation of nitrophenols: A comparative study. *Chemosphere* **2002**, *46* (6), 913−922.

(11) Kwon, B. G.; Lee, D. S.; Kang, N.; Yoon, J. Characteristics of *p*-chlorophenol oxidation by Fenton's reagent. *Water Res.* **1999**, *33* (9), 2110−2118.

(12) Basu, S.; Wei, I. W. Mechanism and kinetics of oxidation of 2,4,6-trichlorophenol by Fenton's Reagent. *Environ. Eng. Sci.* **2000**, *17* (5), 279−290.

(13) Kavitha, V.; Palanivelu, K. Degradation of 2-chlorophenol by Fenton and photo-Fenton proceses. A comparative study. *J. Environ. Sci. Health, Part A* **2003**, *38* (7), 1215−1231.

(14) Beltran de Heredia, J.; Dominguez, J. R.; Peres, J. A. Eliminación de compuestos fenólicos por oxidación avanzada. Estimación de costes. *Ing. Quim.* **2002**, *386*, 142−146.

(15) Pérez, M.; Torrades, F.; García-Hortal, J. A.; Doménech, X.; Peral J. Removal of organic contaminants in paper pulp treatment effluents under Fenton and photo-Fenton conditions. *Appl. Catal., B* **2002**, *36* (1), 63−74.

(16) Chen, R.; Pignatello, J. J. Role of quinone intermediates as electron shuttles in Fenton and photoassisted Fenton oxidations of aromatic compounds. *Environ. Sci. Technol.* **1997**, *31* (8), 2399−2406.

(17) Beltran de Heredia, J.; Torregrosa, J.; Domínguez, J. R.; Peres, J. A. Kinetic model for phenolic compound oxidation by Fenton's reagent. *Chemosphere* **2001**, *45* (1), 85−90.

(18) Kang, N.; Lee, D. S.; Yoon, J. Kinetic modeling of Fenton oxidation of phenol and monochlorophenols. *Chemosphere* **2002**, *47* (9), 915−924.

(19) Rivas, F. J.; Beltran, F. J.; Frades, J.; Buxeda, P. Oxidation of *p*-hydroxybenzoic acid by Fenton's reagent. *Water Res.* **2001**, *35* (2), 387−396.

(20) Al-Hayek, N.; Eymery, J. P.; Doré, M. Catalytic oxidation of phenols with hydrogen peroxide. *Water Res.* **1985**, *19* (5), 657−666.

(21) Andreozzi, R.; Caprio, V.; Insola, A.; Marotta, R. Advanced oxidation processes (AOP) for water purification and recovery. *Catal. Today* **1999**, *53* (1), 51−59.

(22) Santos, A.; Yustos, P.; Quintanilla, A.; García-Ochoa, F.; Casas, J. A.; Rodriguez, J. J. Evolution of toxicity upon wet catalytic oxidation of phenol. *Environ. Sci. Technol.* **2004**, *38*, 133−138.

(23) Eisenberg, G. M. Colorimetric determination of hydrogen peroxide. *Ind. Eng. Chem. Anal.* **1943**, *15* (5), 327−328.

(24) Alnaizy, R.; Akgerman, A. Advanced oxidation of phenolic compounds. *Adv. Environ. Res.* **2000**, *4*, 233−244.

(25) Eisenhauer, H. R. Oxidation of phenolic wastes. *J. Water Pollut. Control Fed.* **1964**, *36*, 1116−1128.

(26) Alegría, Y.; Liendo, F.; Nuñez, O. On the Fenton degradation mechanism. The role of oxalic acid. *Arkivoc* **2003**, *10*, 538−549.

(27) Scott, A. I. *Interpretation of the Ultraviolet Spectra of Natural Products*; Pergamon: Oxford, U. K., 1964.

(28) Scheck, C. K.; Frimmel, F. H. Degradation of phenol and salicylic acid by ultraviolet radiation/hydrogen peroxide/oxygen. *Water Res.* **1995**, *29* (10), 2346−2352.